

CORONARY ANGIOGRAPHY

Spiral Magnetic Resonance Coronary Angiography—Direct Comparison of 1.5 Tesla vs. 3 Tesla

Phillip C. Yang, M.D.,^{1,*} Patricia Nguyen, M.D.,¹
Ann Shimakawa, Ph.D.,³ Jean Brittain, Ph.D.,³ John Pauly, Ph.D.,²
Dwight Nishimura, Ph.D.,² Bob Hu, M.D.,²
and Michael McConnell, M.D., M.S.E.E.¹

¹Department of Medicine, Division of Cardiovascular Medicine and ²Magnetic Resonance Systems Research Laboratory, Department of Electrical Engineering, Stanford University, Stanford, California, USA

³General Electric Medical Systems, Menlo Park, California, USA

ABSTRACT

Background. MR coronary angiography (MRCA) has been demonstrated successfully at 3 Tesla (T). However, the advantages remain unclear. No systematic comparison of MRCA between 1.5 T and 3 T has been performed. Therefore, anatomic coverage, image quality, signal-to-noise ratio (SNR), contrast-to-noise ratio (CNR), and susceptibility artifacts were compared in 23 subjects. *Methods and Results.* Identical real-time (RT) and high-resolution (HR) sequences were implemented on the GE 1.5 T (Signa Twinspeed) and 3.0 T (Signa VH/i) whole body systems (GE, Milwaukee, WI). Both scanners were equipped with high-performance gradient systems capable of 40 mT/m peak amplitude and 150 mT/m/ms slew rate. Real-time localization of the coronary arteries was followed by a cardiac-gated, breath-hold HR sequence. Twenty-three subjects were recruited consecutively and underwent both 3 T and 1.5 T MRCA within one week. Coronary coverage based on the number of coronary segments visualized, image quality using a grading scale, SNR, CNR, and presence of susceptibility artifacts were analyzed. A significant improvement in SNR (47%), CNR (30%), and image quality were seen in 3 T. However, a significant increase in susceptibility artifacts was also noted. *Conclusion.* MRCA at 3 T significantly improves SNR, CNR, and image quality at the expense of susceptibility artifacts.

*Correspondence: Phillip C. Yang, M.D., Stanford University School of Medicine, 300 Pasteur Drive, Room H-2157, Stanford, CA 94305-5233, USA; Fax: (650) 724-4034; E-mail: pyang@cvmed.stanford.edu.

Further optimization of the imaging parameters at 3 T may facilitate clinical implementation of MRCA.

Key Words: Magnetic resonance imaging; Coronary arteries.

CONDENSED ABSTRACT

Successful MRCA at 3 T has been demonstrated. However, the advantages of MRCA at this higher field strength remain unclear. Therefore, a systematic comparison of MRCA at 3 T and 1.5 T was performed. Anatomical coverage, image quality, SNR, CNR, and susceptibility artifact were analyzed in 23 subjects. The overall SNR, CNR, and image quality were improved for MRCA at 3 T. With further optimization, high field imaging of the coronary arteries may benefit clinical implementation of MRCA.

INTRODUCTION

Clinical implementation of magnetic resonance coronary angiography (MRCA) remains problematic. The coronary arteries are small and tortuous, spanning multiple imaging planes. The vessels are embedded in tissue with competing MR signals from fat, myocardium, and underlying ventricular blood. Moreover, asynchronous cardiac and respiratory motions provide significant challenges. Recent clinical studies have reported improved MRCA techniques (Kim et al., 2001; Li et al., 2001; Yang et al., 2003). One of the constraints encountered in these trials, however, is the reduced signal-to-noise ratio (SNR) of the coronary vessels, which limits anatomic coverage, image quality, and detection of coronary stenoses. Successful imaging of coronary arteries at 3 Tesla (T) has been demonstrated to address some of these issues. While high-field MRCA may increase SNR proportionately to the field strength, the advantages of 3 T in coronary artery imaging remain unclear (Dougherty et al., 2001; Jaffer et al., 1996; Wen et al., 1997).

Theoretically, 3 T nearly doubles the SNR when compared to 1.5 T (Wen et al., 1997). The increased SNR should allow improved spatial resolution or reduced scan time (Dougherty et al., 2001). In addition, improved contrast may be achieved by taking advantage of different tissue relaxation times (Noeske et al., 2000). However, a different set of issues arises in high-field MRCA. Susceptibility artifacts due to shorter T_2^* and sensitivity to field inhomogeneity may obscure the vessels located along the heart-lung interface (Noeske

et al., 2000; Reeder et al., 1998). Furthermore, poor radio frequency (RF) penetration, off-resonance effects, and heating limitations may generate additional challenges (Dougherty et al., 2001; Reeder et al., 1998; Stuber et al., 2002; Wen et al., 1997).

In order to analyze the role of 3 T in MRCA, a clinical study was conducted to compare identical MRCA sequence at 1.5 T and 3 T in 23 subjects. Systematic analysis of anatomic coverage, image quality, SNR, CNR, and susceptibility artifacts was performed.

METHODS

Patient Population

A total of 23 subjects (18 volunteers, 5 patients; 18 males, 5 females; age 22 to 70 years; and weight 65 to 124 kg) were enrolled sequentially in the study. Of the five patients suspected of coronary artery disease (CAD), two subjects had known CAD. All 23 subjects underwent MRCA at both 1.5 T and 3 T in a random order within a week. The patients were enrolled from both Stanford and Palo Alto Veterans Affairs Medical Centers. The study protocol was approved by the Human Subjects Committee at Stanford University. All participants gave written informed consent. Patients were ineligible if they had arrhythmias, unstable clinical conditions, coronary artery bypass graft surgery, or contraindications to undergo MRI scan as listed on the screening form.

Protocol

Study patients underwent spiral high resolution (HR) imaging with real-time (RT) localization in the supine position. The RT allowed rapid localization of the four main coronary arteries without any breath holding or cardiac gating. Optimal scan-plane prescription of each coronary artery obtained at end-exhalation position was then saved and transferred to the HR. The HR required cardiac gating using a plethysmogram and breath holding at end exhalation over 20 heartbeats. Multiple slices (5–7), each 5-mm thick, were obtained with each breath hold. In order to standardize surface

coil placement for RT and HR imaging, right sternal-clavicular border was identified. A standard 5-inch diameter surface coil was placed to cover the left chest. Appropriate coverage from the base to the apex of the heart was determined using RT and the coil was moved accordingly. All studies were performed within the SAR limitation.

MR Imaging System

MR Scanner

GE 1.5 T (Signa Twinspeed) and 3.0 T (Signa VH/i) whole body systems (GE, Milwaukee, WI) equipped with high-performance gradient system capable of 40 mT/m peak amplitude and 150 mT/m/ms slew rate were used.

Pulse Sequence

Identical RT and HR sequences were implemented on the 1.5 T and 3 T MR scanners (Kerr et al., 1997; Meyer et al., 1992). The RT sequence (GE, Milwaukee, WI) consisted of a spiral GRE sequence (31 ms TR, 5.2 ms TE, and 30° flip-angle) utilizing a 10-ms spectral spatial pulse and a 16-ms spiral read-out (4 spiral interleaves and 4096 points/interleaf). A frame rate of 5 complete frames/s generated a spatial resolution of 2.25 mm with an FOV of 24 cm. The HR sequence (GE, Milwaukee, WI) consisted of an interleaved spiral GRE (30–50 ms TR/slice, 5.2 ms TE, and 60° flip-angle) utilizing a 10 ms spectral spatial pulse and a 16 ms spiral read-out (18

interleaves and 4096 points). Five to seven slices with 5 mm slice thickness and a 22 cm FOV generated a spatial resolution of $0.75 \times 0.75 \text{ mm}^2$ in 20 heartbeat breath-hold scan. Figure 1 demonstrates the timing diagram and spiral k-space trajectory of HR.

Data Evaluation

All MRCA images at 1.5 T and 3 T were evaluated independently by a total of two observers experienced in MRCA. The MRCA image sets were analyzed using the original MRCA source images. First, the coverage of coronary anatomy was compared based on the number of coronary segments seen in each coronary artery. The coronary segments were identified according to the American Heart Association classification system (Alderman et al., 1993; Austen et al., 1975). Side branches were not included. Second, image quality of each coronary segment was judged using a grading scale based on the extent of the contiguity of the vessel border of a coronary segment (measured in percentage) and the amount of artifact present in the segment (interruption of the vessel border definition) (Yang et al., 2003). The scale ranged from 1 to 4 (1=excellent quality: >91% contiguity of the vessel border of a given segment with minimum artifact; 2=good quality: 75–90% contiguity with minimum to mild artifact; 3=fair quality: 51–74% contiguity with minimum to moderate artifact; and 4=non-diagnostic quality: <50% contiguity). Third, SNR and CNR were calculated in all four coronary arteries. Blood signal was measured as mean signal intensity of the region of interest (ROI) located within the proximal segment of all four coronary arteries. The

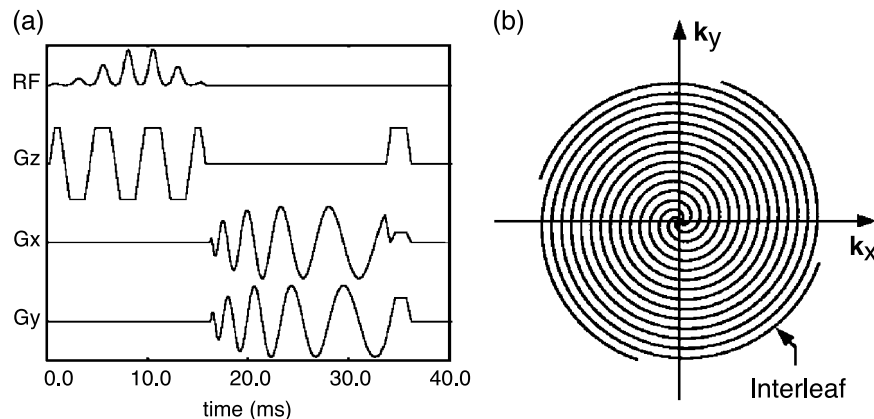


Figure 1. Timing diagram of interleaved spiral sequence demonstrating (a) spectral spatial excitation followed by oscillating gradients in x and y and (b) k-space trajectory.

Table 1. Overall analysis of the coverage of coronary segments, image quality, SNR, CNR, and susceptibility artifacts at 1.5 T and 3.0 T.

	Segments	IQ	SNR	CNR	Susceptibility
1.5 T	163/207 (79%)	2.4 ± 0.7	7.8 ± 3.7	3.3 ± 1.9	0
3.0 T	166/207 (80%)	2.0 ± 0.4	11.5 ± 5.6	4.3 ± 2.9	9
<i>p</i> -value	0.7	<0.001	<0.001	<0.01	<0.005

Abbreviations: NA = not applicable; IQ = image quality (1 = excellent, 2 = good, 3 = fair, and 4 = non-diagnostic); SNR = signal-to-noise ratio; CNR = contrast-to-noise ratio; T = tesla.

standard deviation of noise was estimated as a mean signal intensity of lung air divided by factor of 1.25 (Deshapande et al., 2001; Henkelman, 1985). The myocardial signal was measured as mean signal intensity of the ROI within the left ventricular wall. The SNR and CNR were calculated using the following formulae:

$$\text{SNR} = \text{Blood signal}$$

$$\times 1.25/\text{Air mean image intensity}$$

$$\text{CNR} = (\text{Blood signal} - \text{Myocardial signal})$$

$$\times 1.25/\text{Air mean image intensity}$$

Statistical Analysis

The image quality for the coronary segments was given in mean grade value ± SD. Kappa value was calculated to assess interobserver agreement of image quality. Wilcoxon signed-rank test for matched pairs was employed to determine the presence of significant difference in the image quality of the coronary arteries between 1.5 T and 3 T. A paired, two-tailed Student T-Test was performed to determine the presence of significant difference in the anatomical coverage, SNR, CNR, and susceptibility artifacts of the coronary arteries between 1.5 T and 3 T. A *p*-value less than 0.05 was considered significant.

RESULTS

Coverage of Coronary Anatomy

A total of 414 coronary segments were analyzed. At 1.5 T, 79% (163/207) of the coronary segments were seen, while at 3 T, 80% (166/207) of the segments were visualized. No significant improvement in coronary coverage was seen at 3 T. Table 1 summarizes the overall coverage of the coronary anatomy. Table 2 details the number of coronary segments visualized in each coronary artery.

Image Quality of the Coronary Segments

An overall analysis of the image quality of the coronary anatomy demonstrated significant improvement at 3T. The mean image quality at 1.5 T and 3 T were 2.4 and 2.0 (*p* < 0.001), respectively. Subgroup analysis of individual coronary arteries demonstrated significant improvement of image quality of LCx and LAD (*p* < 0.05). Other arteries demonstrated a non-significant trend toward improved image quality. When each coronary artery was divided into coronary segments, the analysis of individual coronary segments demonstrated that excellent to good (1–2) image quality was obtained in 66% (137/207) and 74% (154/207) of the segments at 1.5 T and 3 T, respectively. Fair

Table 2. Total number of coronary segments visualized at 1.5 T and 3.0 T.

	RCA		LM		LAD		LCx	
	1.5 T	3.0 T						
Proximal	23/23	23/23	22/23	22/23	23/23	22/23	23/23	23/23
Middle	21/23	22/23	NA	NA	22/23	23/23	NA	NA
Distal	19/23	16/23	NA	NA	10/23	12/23	0/23	3/23
Total	63/69	61/69	22/23	22/23	55/69	57/69	23/46	26/46

Abbreviations: NA = not applicable; RCA = right coronary artery; LM = left main artery; LAD = left anterior descending artery; LCx = left circumflex artery.

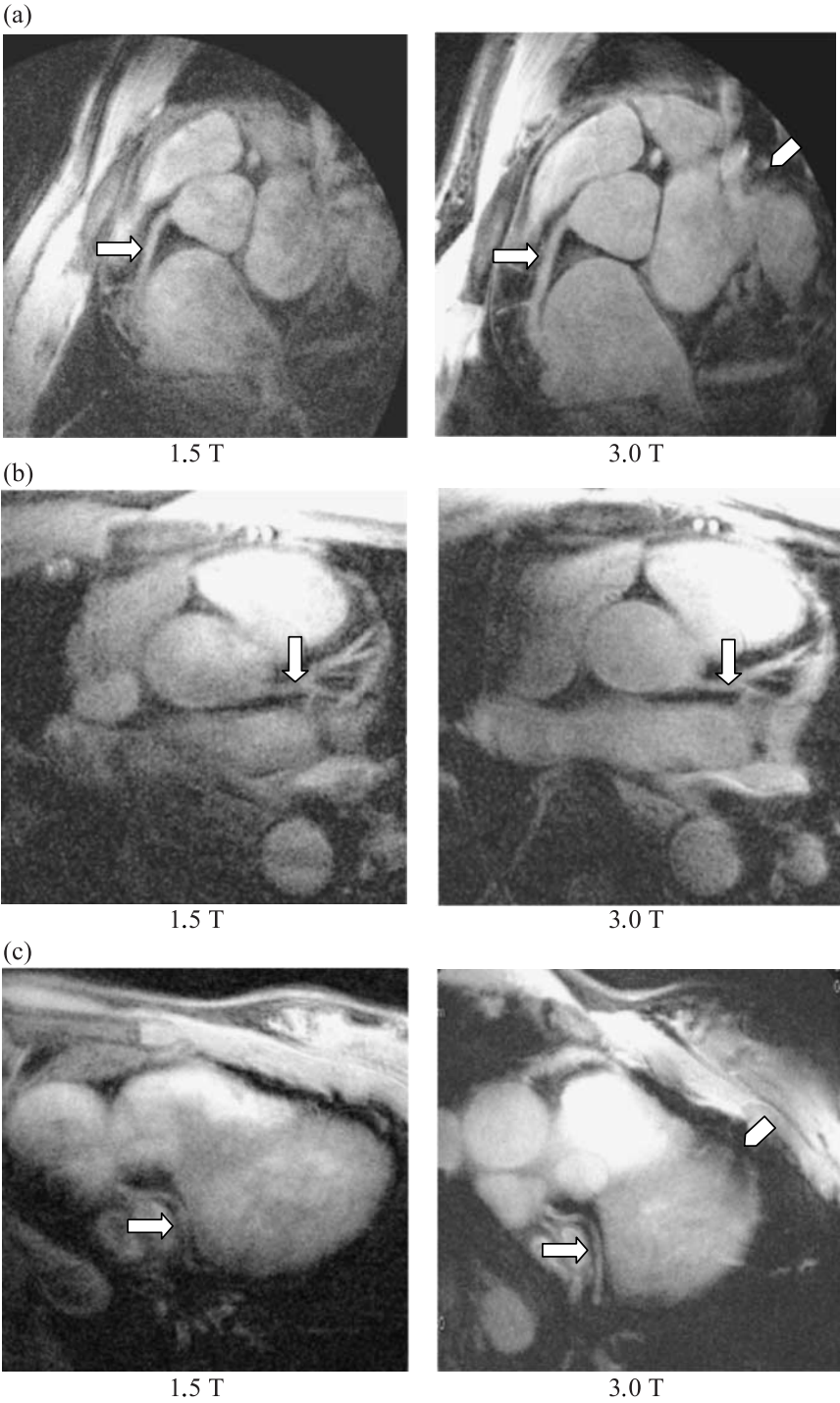


Figure 2. Representative spiral MRCA images and susceptibility artifacts (a) right coronary artery (RCA), (b) left main (LM) and left anterior descending artery (LAD), and (c) left circumflex artery (LCx). The coronary arteries at 1.5 T and 3 T are designated with a white block arrow and susceptibility artifacts are indicated with a white block arrowhead.

Table 3. Mean image quality, SNR, CNR, and presence of susceptibility artifacts in the individual coronary arteries at 1.5 T and 3.0 T.

	IQ		SNR		CNR		Susceptibility	
	1.5 T	3.0 T	1.5 T	3.0 T	1.5 T	3.0 T	1.5 T	3.0 T
RCA	2.0	1.9	8.3	12.5*	4.0	5.7	0	1
LM	1.6	1.2	6.9	11*	3.4	4.3	0	0
LAD	2.2	1.9*	6.8	8.6	2.6	3.4	0	3
LCx	3.0	2.7*	6.1	9.5*	2.1	3.6*	0	5*

Abbreviations: RCA=right coronary artery; LM=left main artery; LAD=left anterior descending artery; LCx=left circumflex artery; IQ=image quality (1=excellent, 2=good, 3=fair, and 4=nondiagnostic); SNR=signal-to-noise ratio; CNR=contrast-to-noise ratio; T=tesla.

* $p < 0.05$.

image quality (grade 3) was obtained in 13% and 6% of all segments at 1.5 T and 3 T, respectively. Nondiagnostic (grade 4) image quality was demonstrated in approximately 21% and 20% of all segments at 1.5 T and 3 T, respectively. The segments graded 3–4 were mostly located in the distal-LCx and -LAD. Interobserver agreement (kappa) in the evaluation of the image quality was 0.81 ($p < 0.05$). Representative images of excellent quality at 1.5 T and 3 T are shown in Fig. 2. Table 1 summarizes the overall mean image quality of the coronary anatomy. Table 3 details the mean image quality of each individual coronary artery at 1.5 T and 3 T.

SNR, CNR, and Susceptibility Artifacts

An overall analysis of SNR and CNR of the coronary anatomy demonstrated significant increase at 3 T. The mean SNR of the coronary arteries at 1.5 T and 3 T were 7.8 and 11.5 ($p < 0.001$), respectively, demonstrating a 47% increase in SNR at 3 T. Subgroup analysis of the SNR of individual coronary arteries demonstrated significant increases of 40%, 56%, and 63% ($p < 0.05$) at RCA, LM, and LCx, respectively. The mean CNR of the coronary segments at 1.5 T and 3 T were 3.3 and 4.4 ($p < 0.005$), respectively, demonstrating significant 36% increase in CNR at 3 T. Subgroup analysis of the CNR of individual coronary arteries demonstrated a significant CNR increase of 71% ($p < 0.05$) of LCx. Table 1 summarizes the overall SNR and CNR of the coronary anatomy. Table 3 details the SNR and CNR of each coronary artery at 1.5 T and 3 T. Finally, susceptibility artifacts were increased significantly at 3 T visualized in 9 subjects and in no subject at 1.5 T ($p < 0.005$). These artifacts were located in the lung-myocardial tissue interface at

mid-RCA, distal-LAD, and LCx regions as shown in Table 3. Subgroup analysis demonstrated that the artifacts were significantly increased in LCx at 3 T ($p < 0.05$). Representative images of susceptibility artifacts are shown in Fig. 2.

DISCUSSION

This is the first clinical study to compare MRCA directly between 1.5 T and 3 T. This study not only demonstrated that spiral MRCA is feasible at 3 T but also provided a comparative assessment of the anatomical coverage, image quality, SNR, CNR, and susceptibility artifacts in 23 subjects. Despite the sensitivity of spiral imaging to off-resonance and field inhomogeneity, the advantages of spiral MRCA at 1.5 T have been reported (Bornert et al., 2001; Keegan et al., 1999; Meyer et al., 1992; Taylor et al., 2000). The studies demonstrated improved spatial and temporal resolution, reduced flow artifact, and higher SNR and CNR. However, it is not known whether this fast imaging technique has similar advantages at 3 T. The known sensitivity of spiral technique to rapid T_2^* decay, off-resonance spin, and field inhomogeneity artifacts may potentially limit its use at 3 T (Meyer et al., 1992; Reeder et al., 1998).

This study demonstrated that spiral MRCA at 3 T generated significant improvement in the overall SNR, CNR, and image quality of the coronary anatomy. Analysis of individual coronary arteries demonstrated significant increase in SNR of RCA, LM, and LCx. Similarly, CNR increased significantly at LCx. The LCx, which achieved both improved SNR and CNR, showed significant improvement in its image quality. This finding is consistent with the prior MRCA trials in which LCx has been the most difficult vessel to image

due to inadequate SNR and CNR (Kim et al., 2001; Li et al., 2001; Yang et al., 2003). Thus, the increased SNR and CNR provided by 3 T at LCx provided significant improvement in the image quality. The LAD, which achieved nonsignificant trend toward improved SNR and CNR, also demonstrated significant improvement in its image quality. This finding suggests that LM and RCA with statistically improved SNR and trend toward increased CNR may demonstrate improved image quality with larger sample size. The analysis of anatomical coverage demonstrated no significant difference. Increased overall susceptibility artifacts seen in almost half of the subjects may in part explain this limitation, especially in the distal segments of the coronary arteries near the tissue interface. Although this study indicates a potential benefit of spiral MRCA at 3 T, a careful examination of the data suggests a need for a more methodical optimization of the imaging sequences to fully exploit the benefits of 3 T to achieve improved image quality in all coronary arteries and to increase anatomical coverage. Carefully optimized receiver coil, echo time (TE), RF pulse, and acquisition strategy should enhance imaging of the coronary arteries (Noeske et al., 2000; Taylor et al., 2000; Wen et al., 1997).

Several receiver coil designs were optimized for 3 T cardiac fast gradient echo sequences (Noeske et al., 2000). They were small single coil (23 cm × 17 cm), small dual phased-array coil, large dual quadrature-array coil (33 cm × 27 cm), and large dual phased-array coil. The small dual coil generated the highest SNR in all regions of the heart and represented an optimal compromise between sensitivity volume and SNR for cardiac imaging.

At 3 T, long TE, suboptimal RF pulse, and inefficient read-out strategy increase the susceptibility to field inhomogeneity, off-resonance, and T_2^* effects. Echo time longer than 20 ms has resulted in substantial flow artifacts at 3T (Wen et al., 1997). Reported measurements of T_2^* in the heart at 1.5 T range mostly from 30–40 ms, although in the apex it decreases to as much as 12 ms (Reeder et al., 1998). The T_2^* effects, expected to be more pronounced at 3 T, explain the increased susceptibility artifacts seen in this study. Pulse sequences designed with a shorter TE will reduce the severity of this artifact. The RF pulses must also be redesigned to account for the induced conductive and dielectric currents and phase variation of the RF field across the body due to the longer RF wavelength and shorter RF penetration in 3 T (Wen et al., 1997). The doubled frequency shift between water and fat will enable a shorter RF pulse duration to reduce TE and TR, thereby minimizing flow artifact and T_2^* signal

loss. Another important modification is the optimization of the spiral readout. The blurring from off-resonance spins and T_2^* effects during the relatively long readouts are more problematic at 3 T (Meyer et al., 1992; Reeder et al., 1998). Shorter readout in 8–10 ms range or the use of variable-density spirals may mitigate the artifacts although some trade-off may occur due to increased aliasing and reduced SNR (Lee et al., 2001).

CONCLUSION

A clinical study directly comparing spiral MRCA at 1.5 T and 3 T has been performed. The coronary images at 3 T demonstrated improved SNR and CNR with subsequent improvement in the image quality. The findings from this study suggest that a methodical optimization of TE, RF pulse, and spiral readout will further enhance the use of higher field in MRCA. These improvements may enable routine clinical implementation of spiral MRCA at 3 T.

ACKNOWLEDGMENTS

This study was supported by grants 5K23 HL04338-02 and HL39297 from the National Heart, Lung, and Blood Institute of NIH; GE Medical Systems; and the Donald W. Reynold Clinical Cardiovascular Research Center at Stanford University.

REFERENCES

- Alderman, E., Corley, S., Fisher, L., Chaitman, B., Faxon, D., Foster, E., Killip, T., Sosa, J., Bourassa, M. (1993). Five-year angiographic follow-up of factors associated with progression of coronary artery disease in the Coronary Artery Surgery Study (CASS). *J. Am. Coll. Cardiol.* 22:1141–1154.
- Austen, W., Edwards, J., Frye, R., Gensini, G., Gott, V., Griffith, L., McGoon, M., Murphy, M., Roe, B. (1975). A reporting system on patients evaluated for coronary artery disease. Report of the ad hoc committee for grading coronary artery disease, council on cardiovascular surgery, American heart association. *Circulation* 51:5–40.
- Bornert, P., Stuber, M., Botnar, R., Kissinger, K., Koken, P., Spuentrup, E., Manning, W. (2001). Direct comparison of 3D spiral vs. cartesian gradient-echo coronary magnetic resonance angiography. *Magn. Reson. Med.* 46:789–794.

- Deshapande, V., Shea, S., Laub, G., Simonetti, O., Finn, J., Li, D. (2001). 3D magnetization-prepared true-FISP: a new technique for imaging coronary arteries. *Magn. Reson. Med.* 46:494–502.
- Dougherty, L., Connick, T., Mizsei, G. (2001). Cardiac imaging at 4 Tesla. *Magn. Reson. Med.* 45:176–178.
- Henkelman, R. (1985). Measurement of signal intensities in the presence of noise in MR images. *Med. Phys.* 12:232–233.
- Jaffer, F., Wen, H., Balaban, R., Wolff, S. (1996). A method to improve the B0 homogeneity of the heart in vivo. *Magn. Reson. Med.* 36:375–383.
- Keegan, J., Gatehouse, P., Taylor, A., Yang, G., Jhooti, P., Firmin, D. (1999). Coronary artery imaging in 0.5-tesla scanner: implementation of real-time, navigator echo-controlled segmented k-space FLASH and interleaved spiral sequences. *Magn. Reson. Med.* 41:392–399.
- Kerr, A., Pauly, J., Hu, B., Li, K., Hardy, C., Meyer, C., Macovski, A., Nishimura, D. (1997). Real-time interactive MRI on a conventional scanner. *Magn. Reson. Med.* 38:355–367.
- Kim, W., Dianas, P., Stuber, M., Flamm, S., Plein, S., Nagel, E., Langerak, S., Weber, O., Pedersen, E., Schmidt, M., Botnar, R., Manning, W. (2001). Coronary magnetic resonance angiography for the detection of coronary stenoses. *N. Engl. J. Med.* 345:1863–1869.
- Lee, J., Hargreaves, B., Nishimura, D. (2001). Fast 3D imaging using variable density spiral trajectories. In: Proceedings of the ISMRM 9th Annual Meeting, Glasgow, Scotland. 1777.
- Li, D., Carr, J., Shea, S., Zheng, J., Deshapande, V., Wielopolski, P., Finn, J. (2001). Coronary arteries: magnetization-prepared contrast-enhanced three-dimensional volume-targeted breath-hold MR angiography. *Radiology* 219:270–277.
- Meyer, C., Hu, B., Nishimura, D., Macovski, A. (1992). Fast spiral coronary artery imaging. *Magn. Reson. Med.* 28:202–213.
- Noeske, R., Seifert, F., Rhein, K., Rinneberg, H. (2000). Human cardiac imaging at 3T using phased array coils. *Magn. Reson. Med.* 44:978–982.
- Reeder, S. B., Faranesh, A. Z., Boxerman, J. L., McVeigh, E. R. (1998). In vivo measurement of T*2 and field inhomogeneity maps in the human heart at 1.5 T. *Magn. Reson. Med.* 39:988–998.
- Stuber, M., Botnar, R., Fischer, S., Lamerichs, R., Smink, J., Harvey, P., Manning, W. (2002). Preliminary report on in vivo coronary MRA at 3 Tesla in humans. *Magn. Reson. Med.* 48:425–429.
- Taylor, A., Keegan, J., Jhooti, P., Gatehouse, P., Firmin, D., Pennell, D. (2000). A comparison between segmented k-space FLASH and interleaved spiral MR coronary angiography sequences. *J. Magn. Reson. Imaging* 11:394–400.
- Wen, H., Denison, T. J., Singerman, R. W., Balaban, R. S. (1997). The intrinsic signal-to-noise ratio in human cardiac imaging at 1.5, 3, and 4 T. *J. Magn. Reson.* 125:65–71.
- Yang, P., Meyer, C., Kerr, A., Terashima, M., Kaji, S., McConnell, M., Macovski, A., Pauly, J., Nishimura, D., Hu, B. (2003). Spiral magnetic resonance coronary angiography with real-time localization. *J. Am. Coll. Cardiol.* 41:1134–1141.

Submitted November 20, 2003

Accepted May 26, 2004